Supplementary

N-Substitution Effects on the Conformations of Iminosugar Analogues of 1-deoxy-L-Idose and 1-deoxy-L-Iduronic Acid.

Lorenzo Taglietti,[a] Eva Palomba,[b] Heiko Lange,[b,d] Luca Zoia,[b] Maria Assunta Chiacchio,[c] Laura Legnani*[a] and Barbara La Ferla*[b]

[a.]Department of Biotechnology and Biosciences, University of Milano-Bicocca, Piazza della Scienza 2, 20126 Milano, Italy.

[b.]Department of Earth and Environmental Science, University of Milano-Bicocca, Piazza della Scienza 1, 20126 Milano, Italy.

[c.]Department of Pharmaceutical and Health Sciences, University of Catania, Viale A. Doria 6, Catania, 95125, Italy

[d.] Biochemical Process Engineering, Division of Chemical Engineering, Department of Civil, Environmental and Natural Resources Engineering, Luleå University Technology, SE-97187 Luleå, Sweden

*Corresponding authors.

Address: Department of Earth and Environmental Science, University of Milano-Bicocca, Piazza della Scienza 1, 20126 Milano, Italy.
E-mail: barbara.laferla@unimib.it

Address: Department of Biotechnology and Bioscience, University of Milano-Bicocca, Piazza della Scienza 2, 20126 Milano, Italy.
E-mail: laura.legnani@unimib.it

Contents

NMR spectra

(2S,3R,4R,5S)-2-(hydroxymethyl)piperidine-3,4,5-triol, HCl salt (**1**)

^{1}H-NMR, 400 MHz, d_4 MeOD

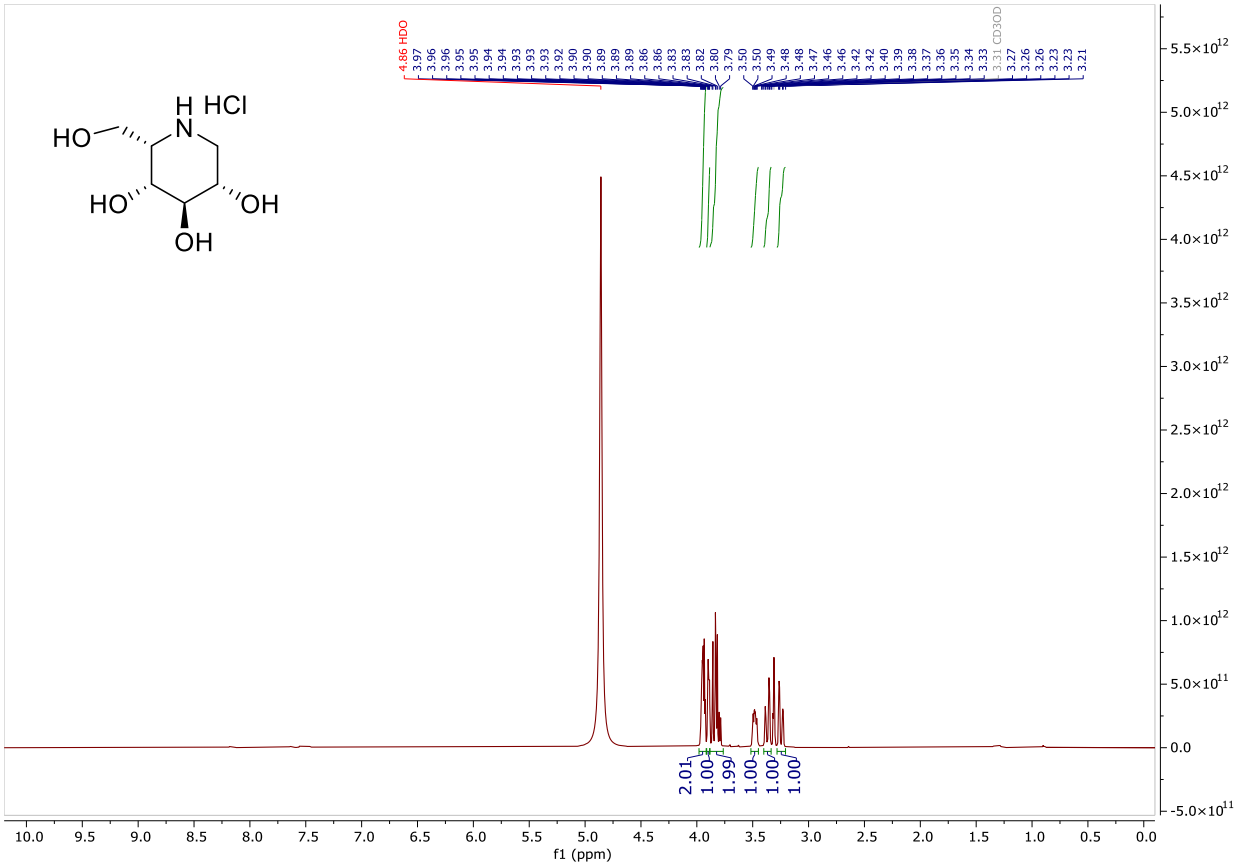

^{13}C-NMR, 101 MHz, d_4 MeOD

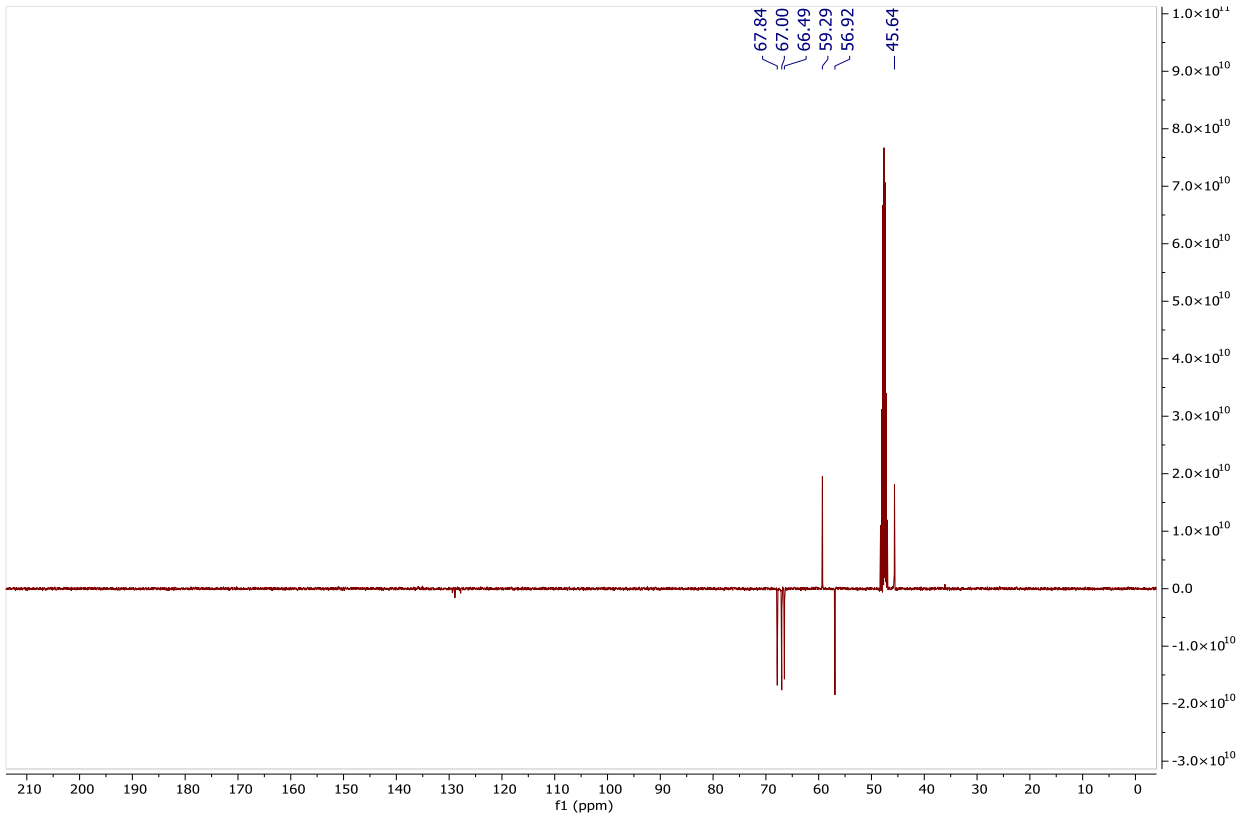

tert-butyl (2S,3R,4R,5S)-3,4,5-trihydroxy-2-(hydroxymethyl)piperidine-1-carboxylate (8)

^{1}H-NMR, 400 MHz, d_4 MeOD

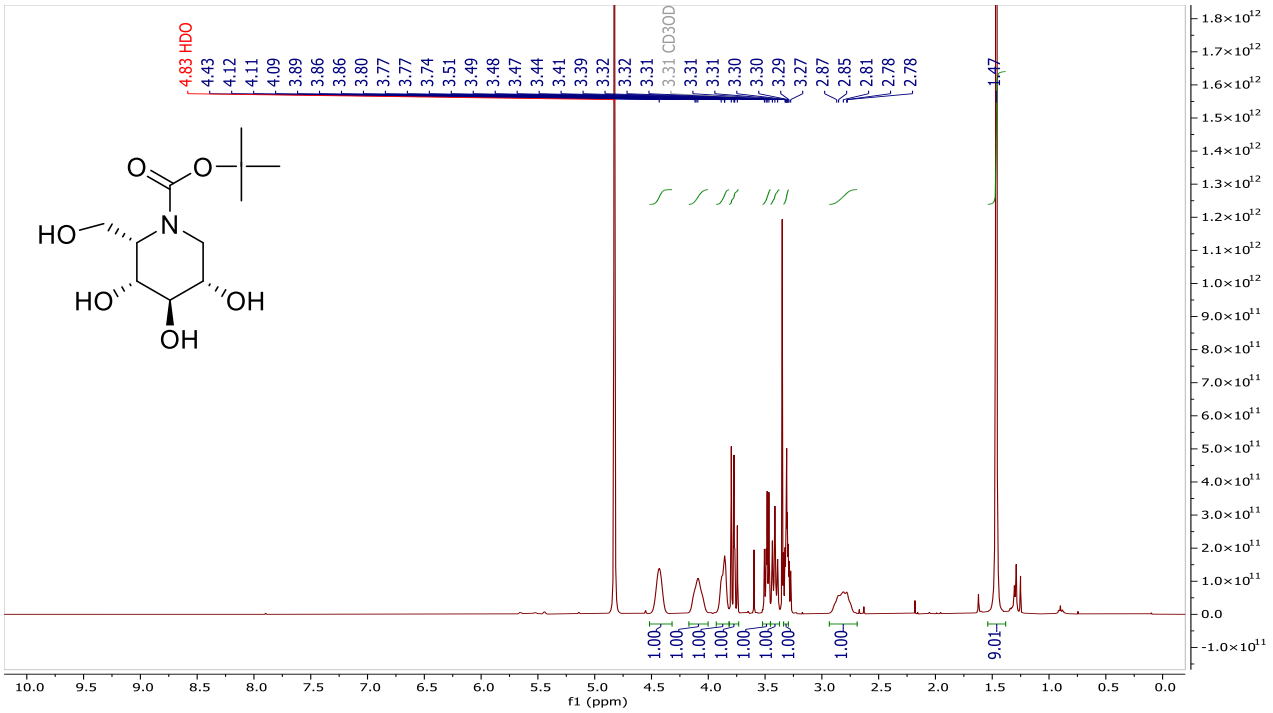

^{13}C-NMR, 101 MHz, d_4 MeOD

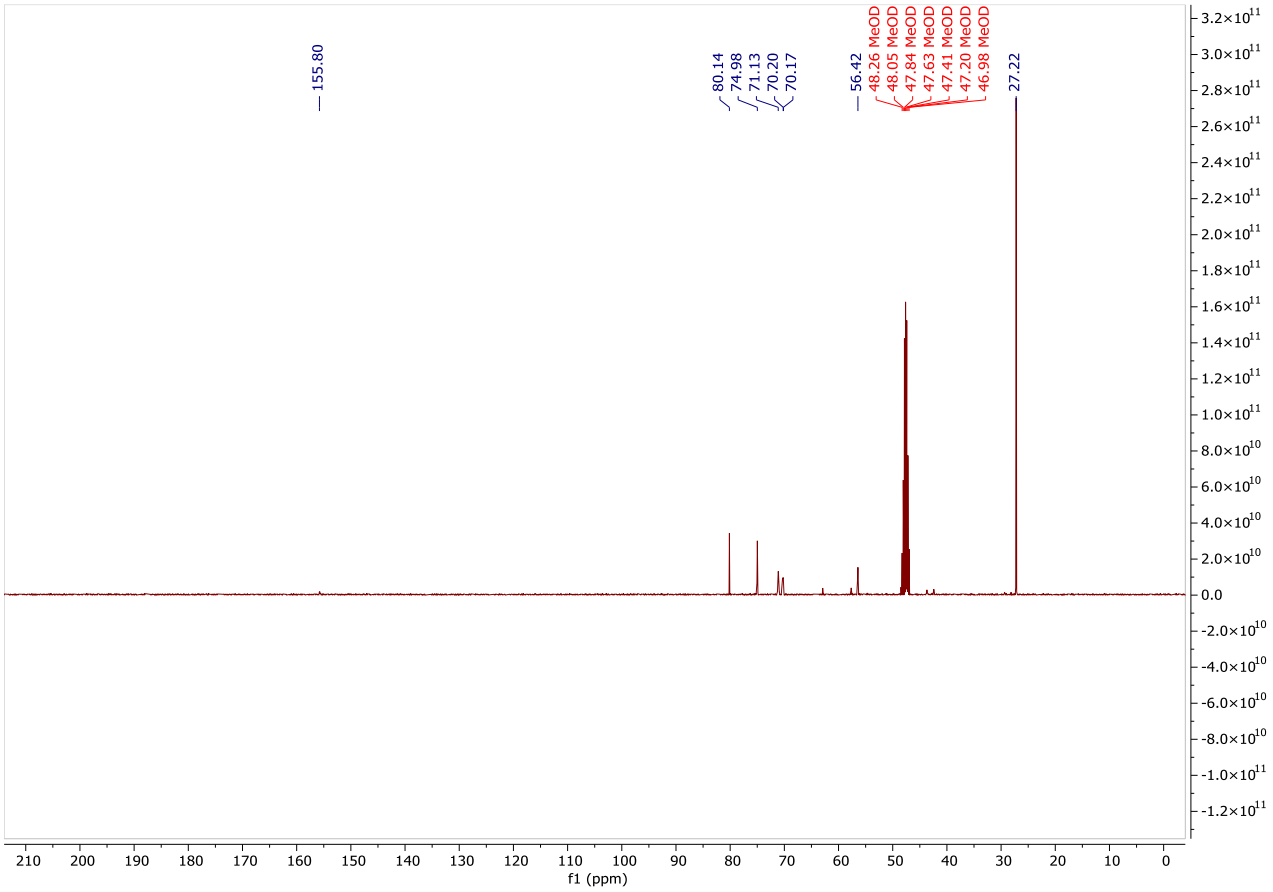

(2R,3R,4R,5S)-3,4,5-trihydroxypiperidine-2-carboxylic acid, HCl salt (2)

^{1}H-NMR, 400 MHz, D_2O

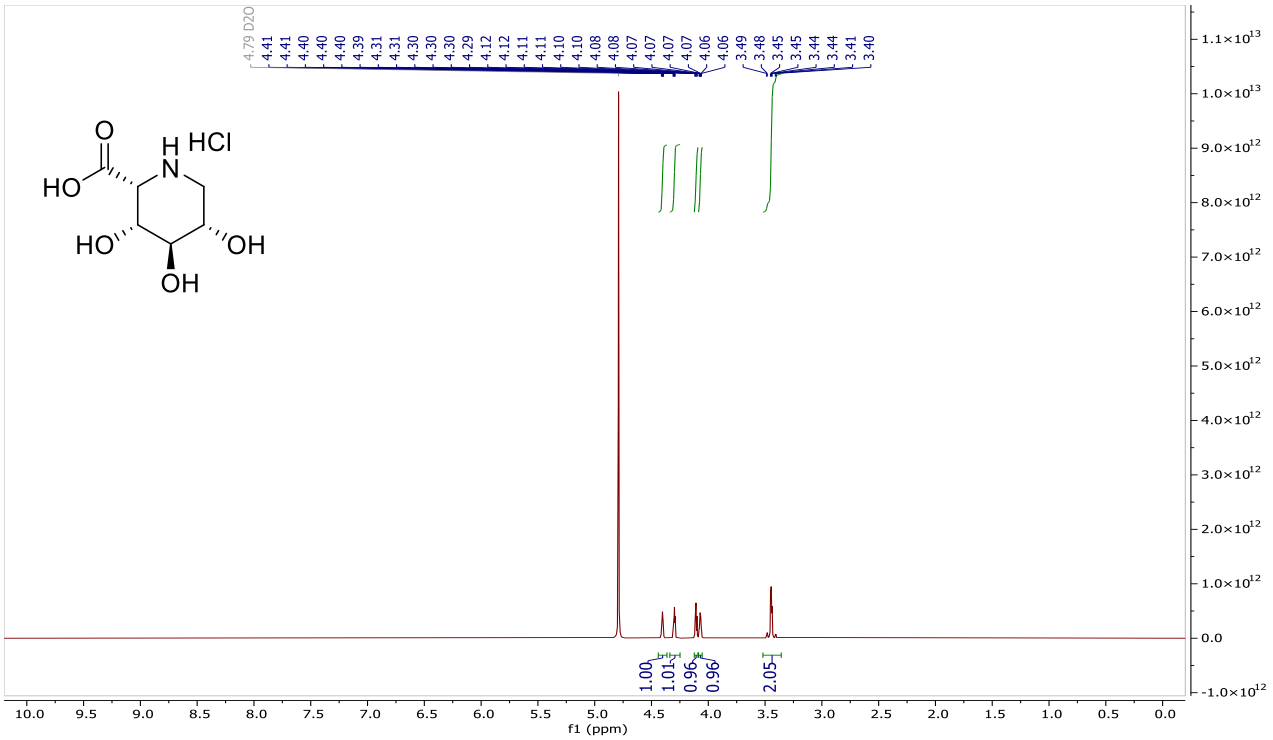

^{13}C-NMR, 101 MHz, D_2O

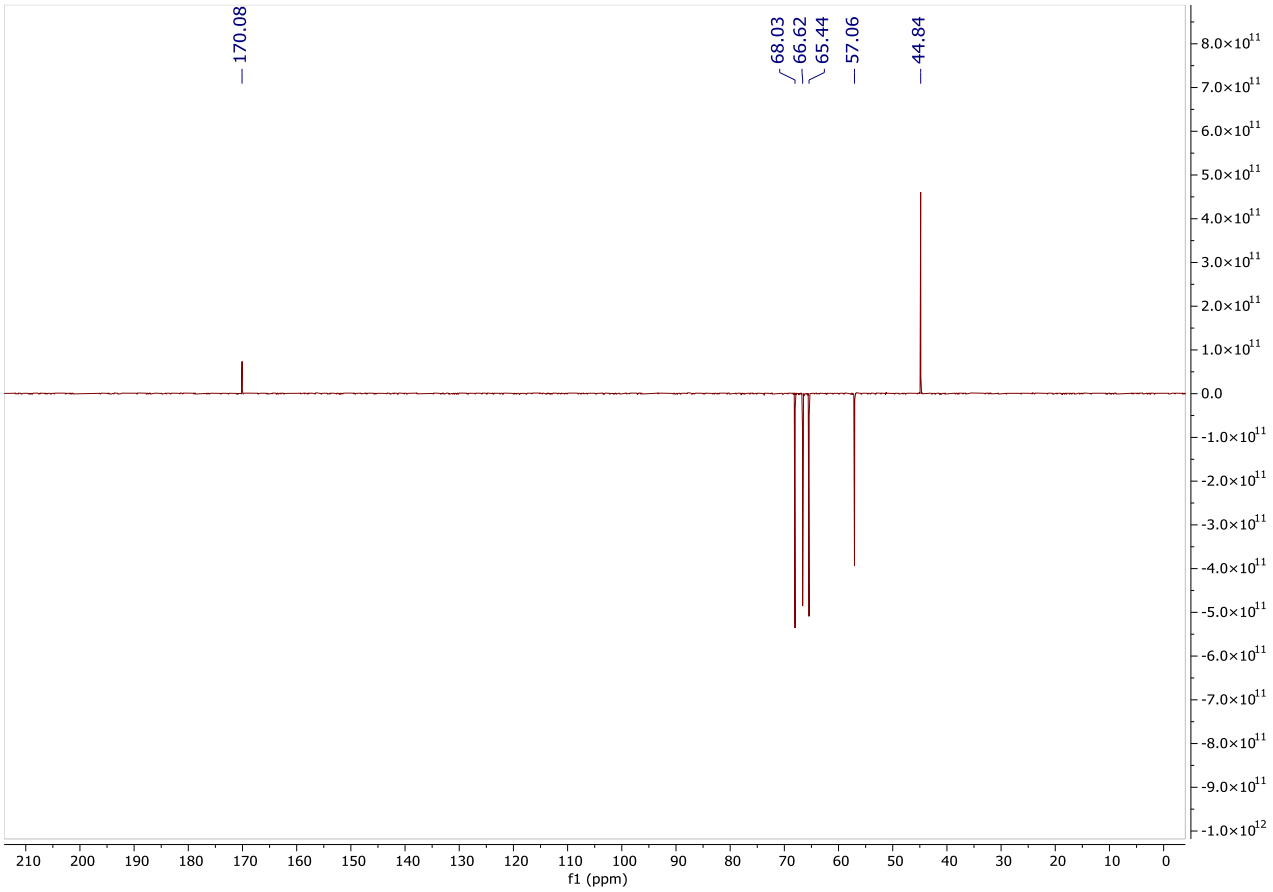

(2R,3R,4R,5S)-1-decyl-3,4,5-trihydroxypiperidine-2-carboxylic acid (4)

^{1}H-NMR, 600 MHz, 310K, D_2O

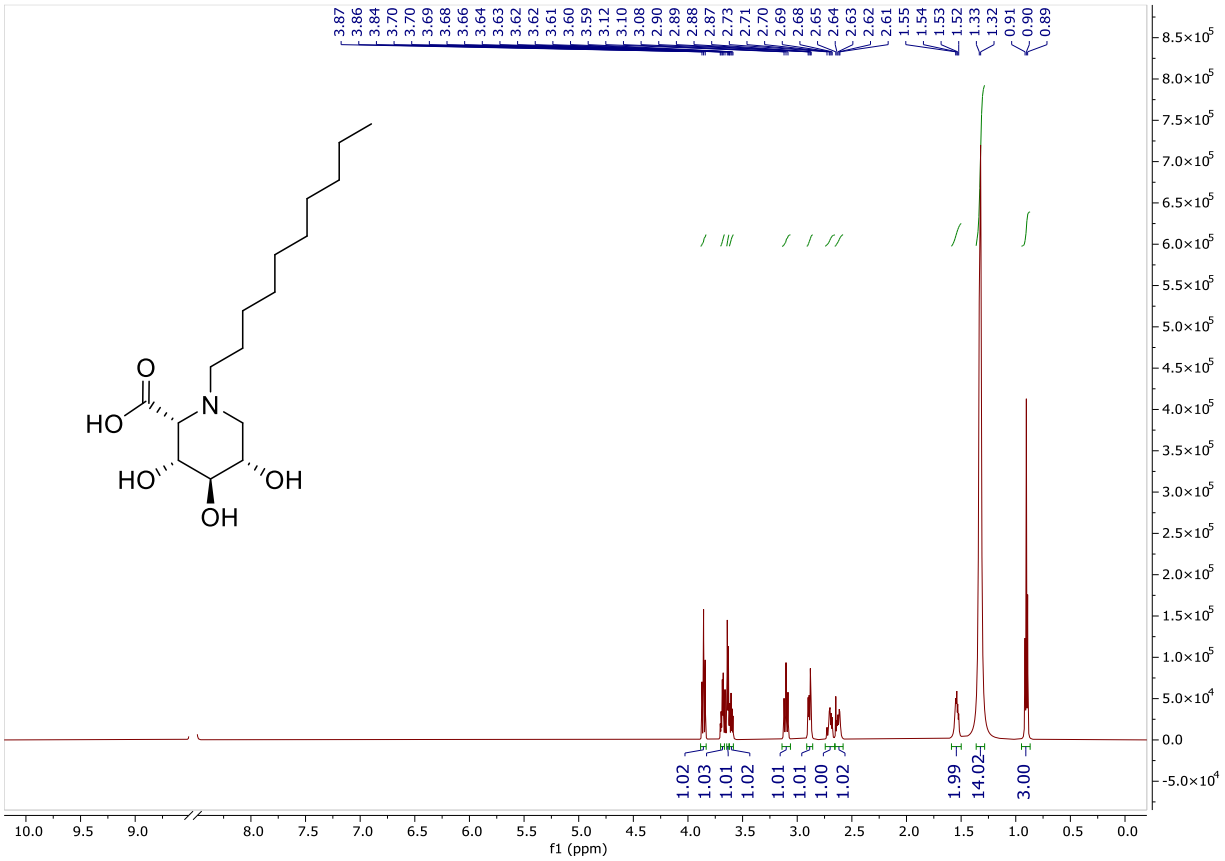

HSQC, 600MHz, D_2O, 310K

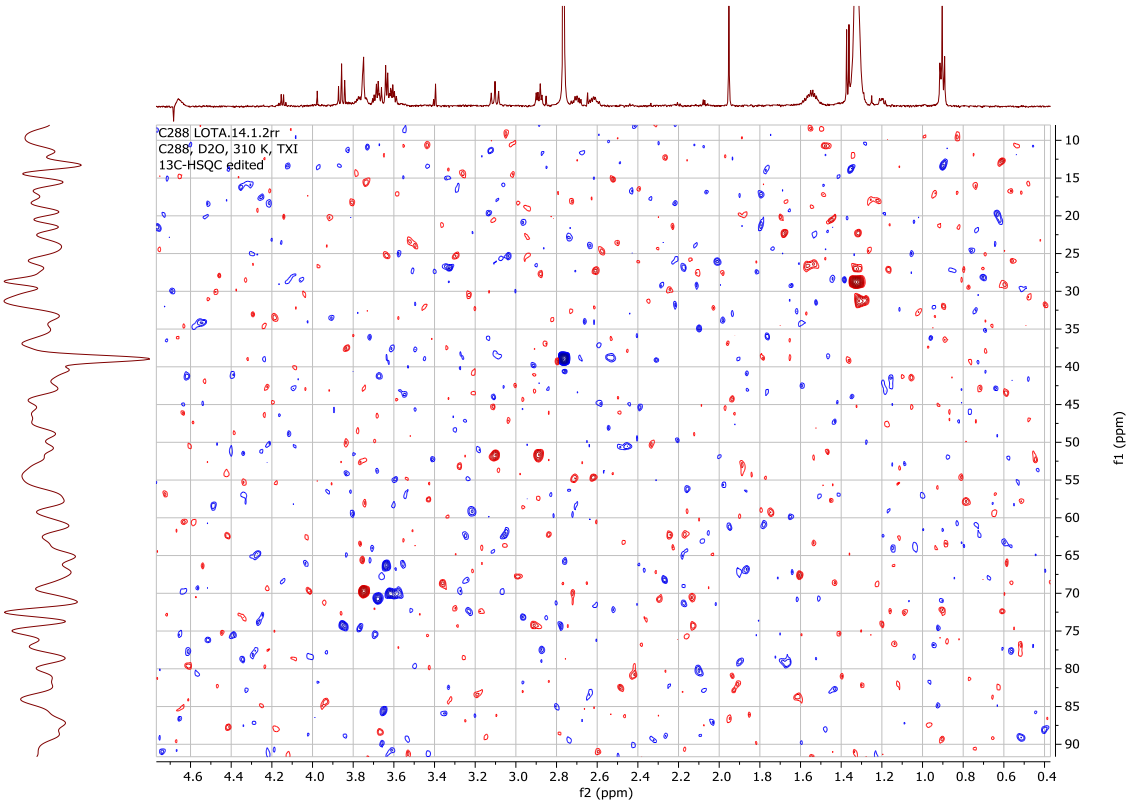

(2S,3R,4R,5S)-3,4,5-tris(benzyloxy)-2-((benzyloxy)methyl)piperidine (9)

^{1}H-NMR, 400 MHz, $CDCl_3$

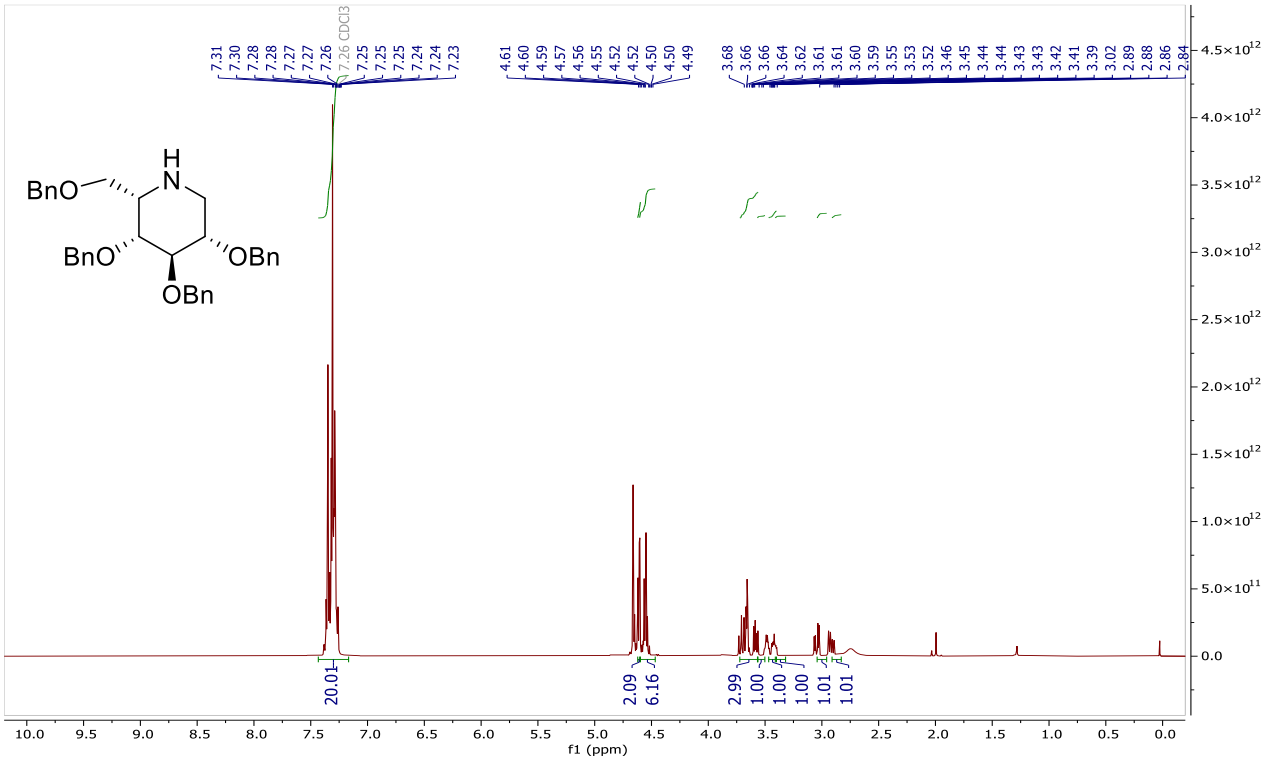

^{13}C-NMR, 101 MHz, $CDCl_3$

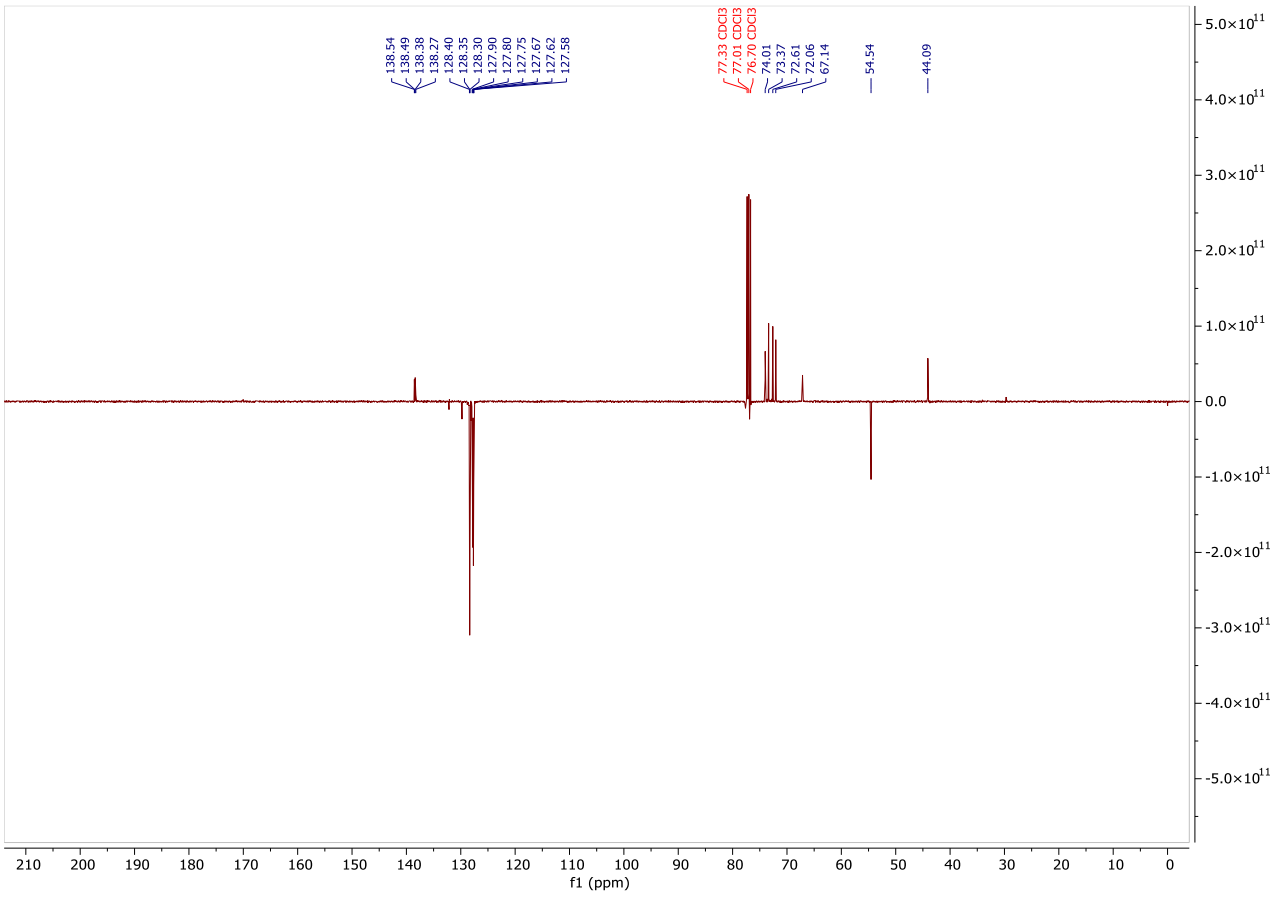

(2S,3R,4R,5S)-3,4,5-tris(benzyloxy)-2-((benzyloxy)methyl)-1-decylpiperidine (10)

^{1}H-NMR, 400 MHz, $CDCl_3$

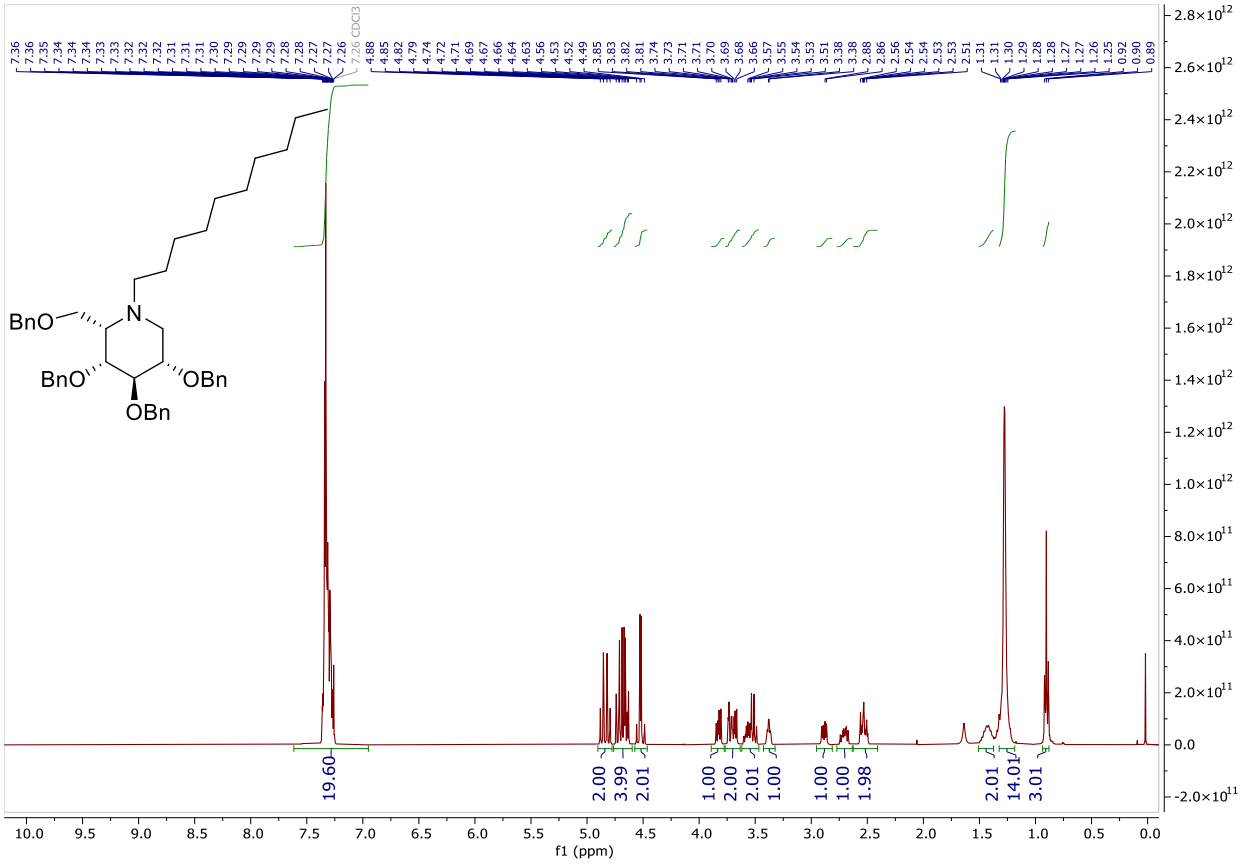

^{13}C-NMR, 101 MHz, $CDCl_3$

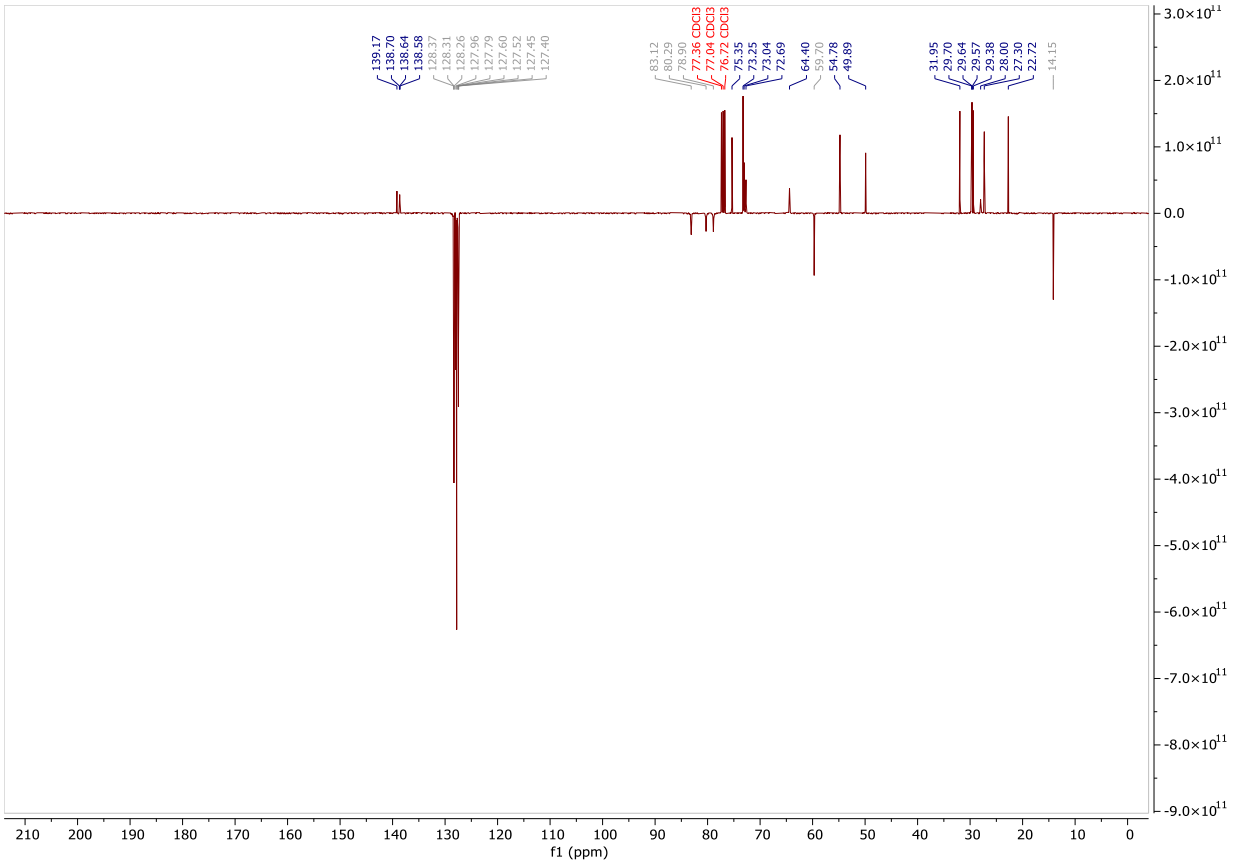

1-((2S,3R,4R,5S)-3,4,5-tris(benzyloxy)-2-((benzyloxy)methyl)piperidin-1-yl)decan-1-one (11)

^{1}H-NMR, 400 MHz, $CDCl_3$

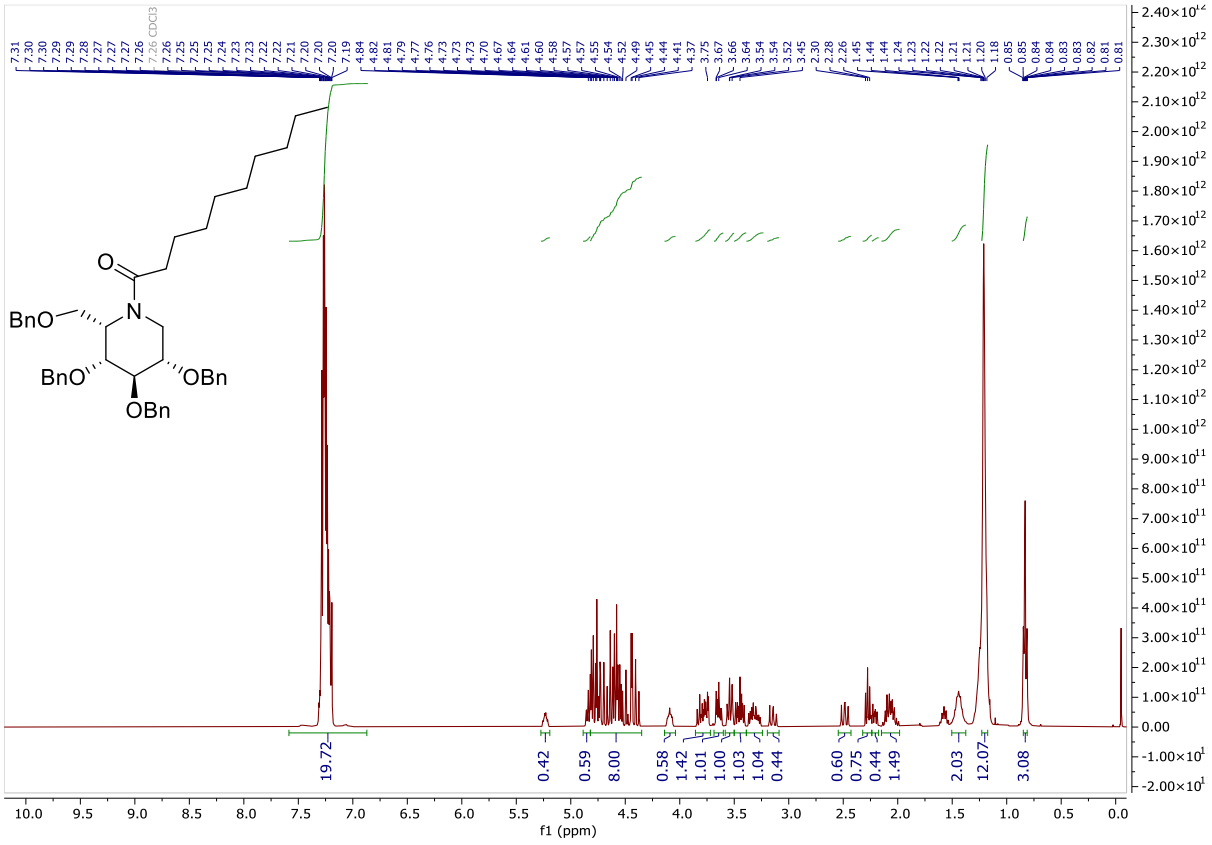

^{13}C-NMR, 101 MHz, $CDCl_3$

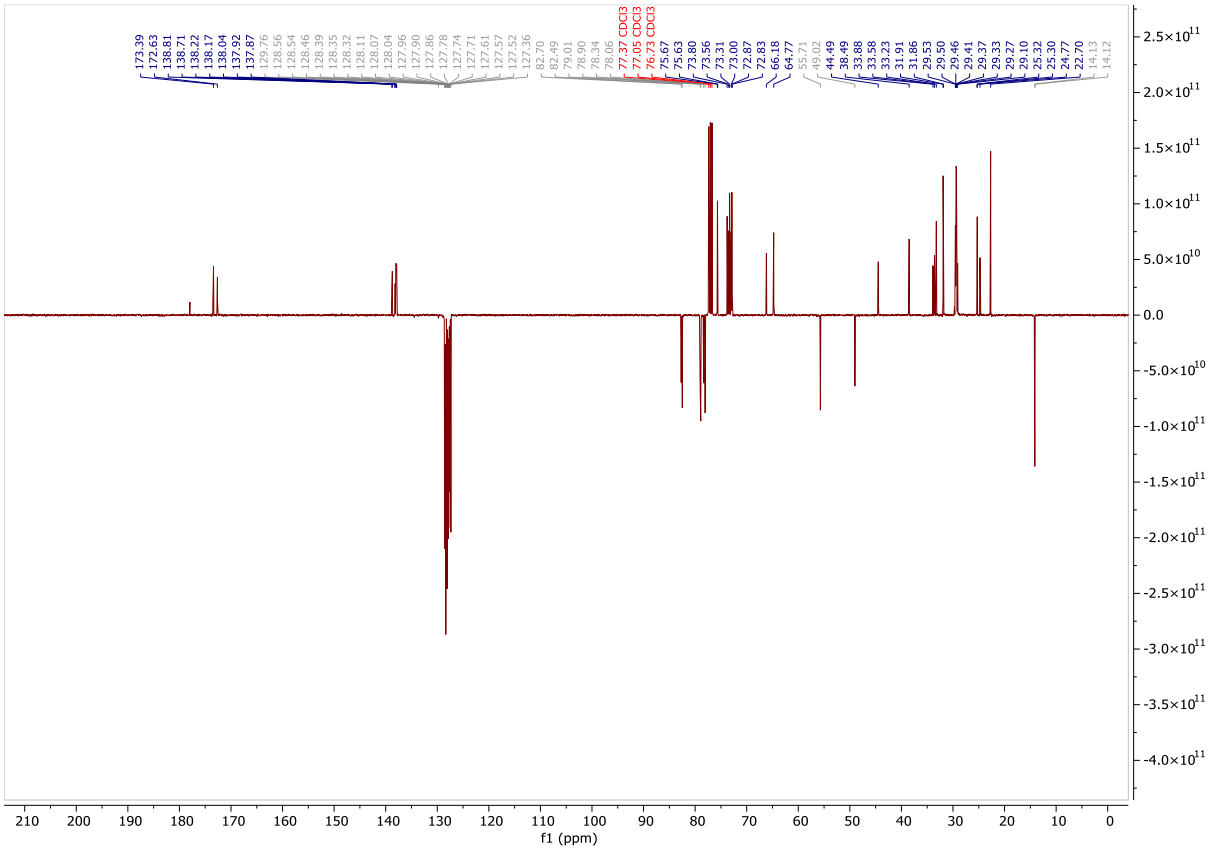

(2S,3R,4R,5S)-1-decyl-2-(hydroxymethyl)piperidine-3,4,5-triol (**3**)

^{1}H-NMR, 400 MHz, d_4 MeOD

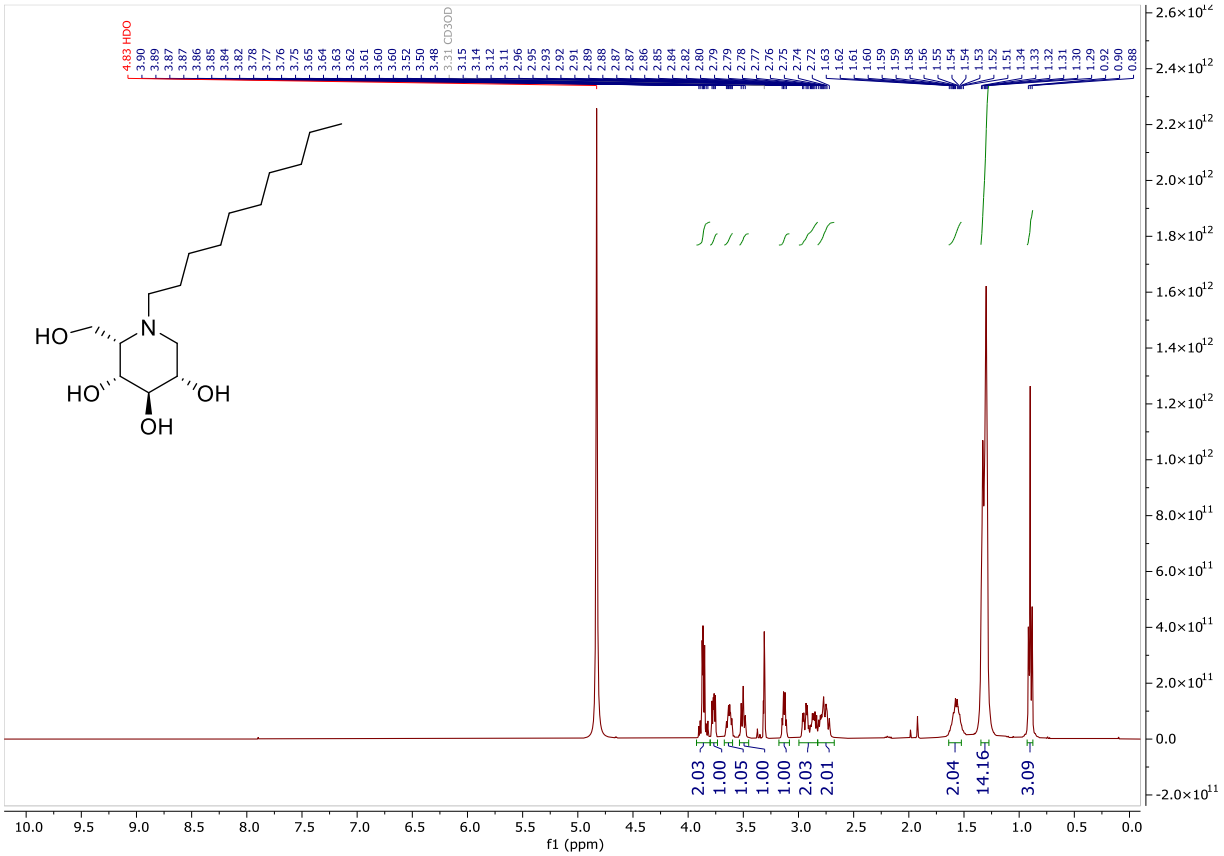

^{13}C-NMR, 101 MHz, d_4 MeOD

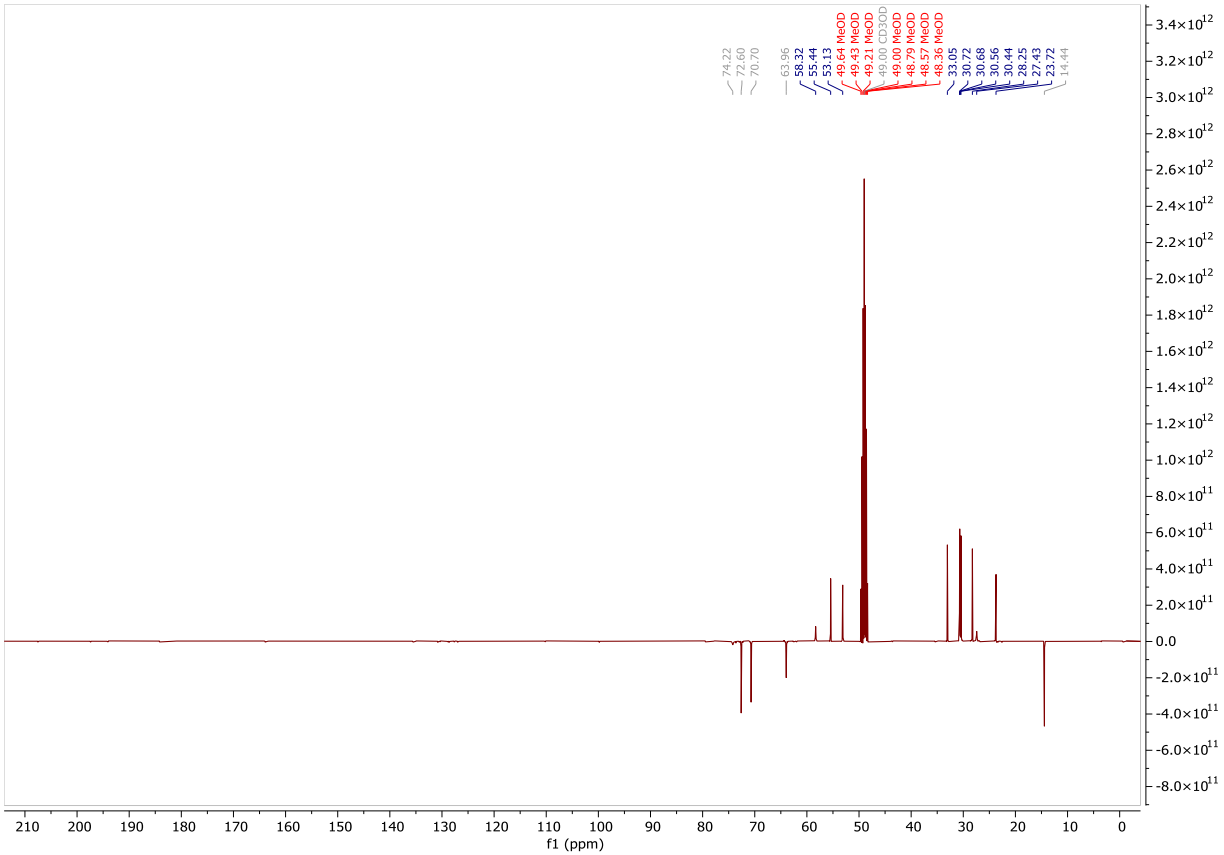

1-((2S,3R,4R,5S)-3,4,5-trihydroxy-2-(hydroxymethyl)piperidin-1-yl)decan-1-one (5)

^{1}H-NMR, 400 MHz, d_4 MeOD

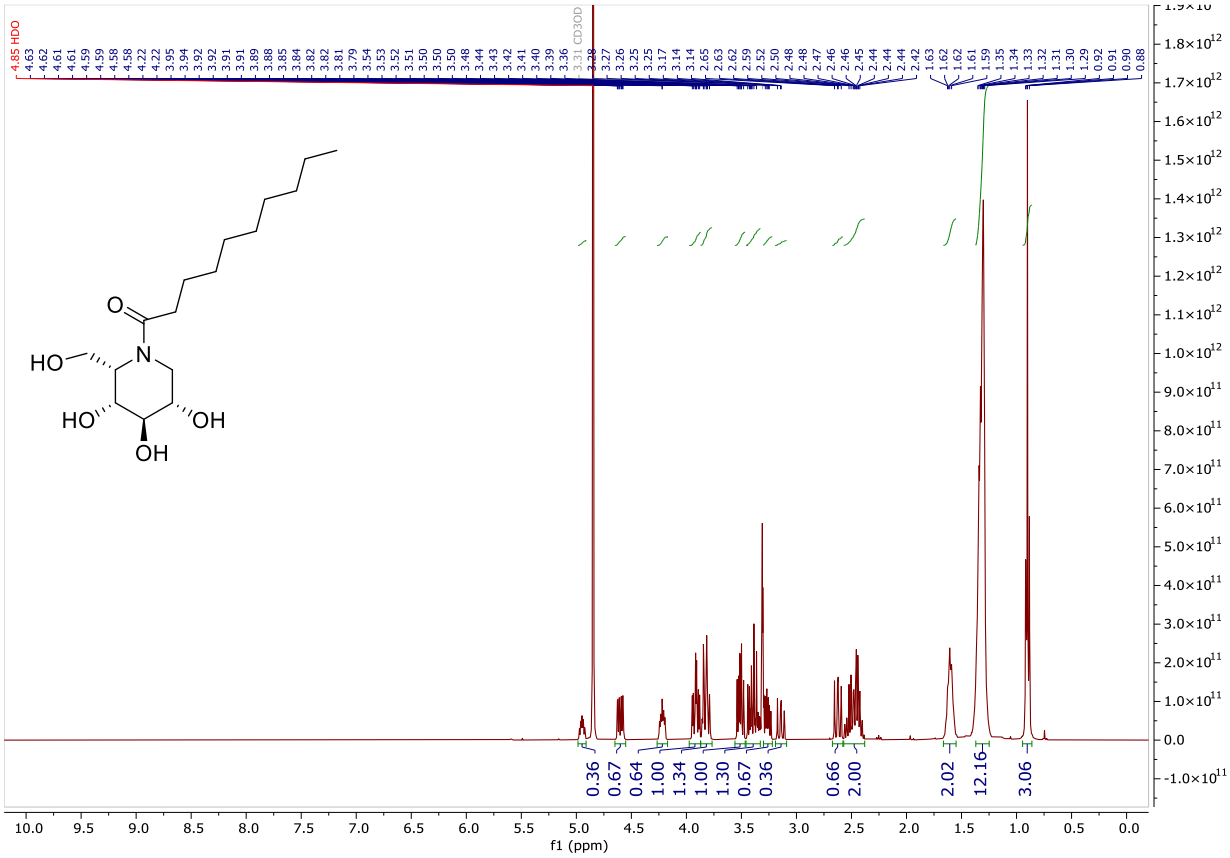

^{13}C-NMR, 101 MHz, d_4 MeOD

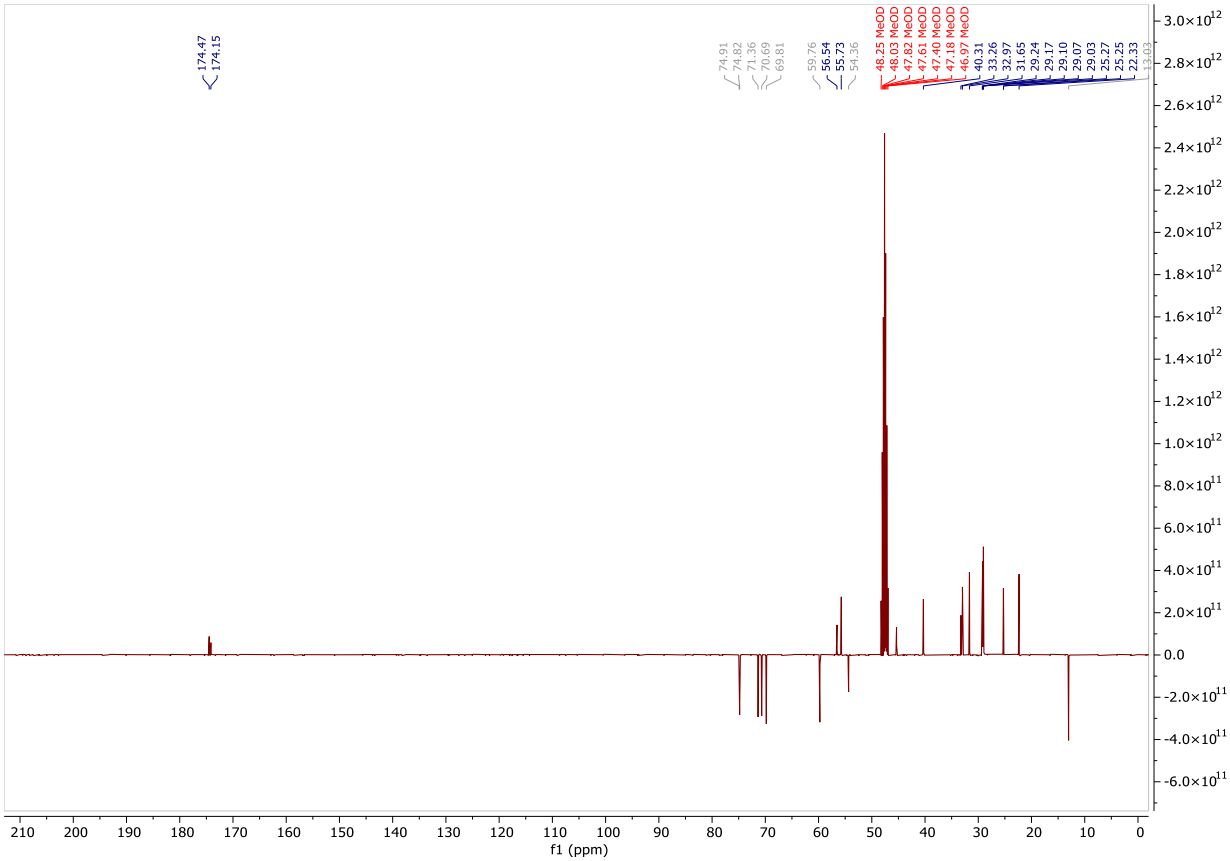

(2R,3R,4R,5S)-1-decanoyl-3,4,5-trihydroxypiperidine-2-carboxylic acid (6)

^{1}H-NMR, 400 MHz, D_2O

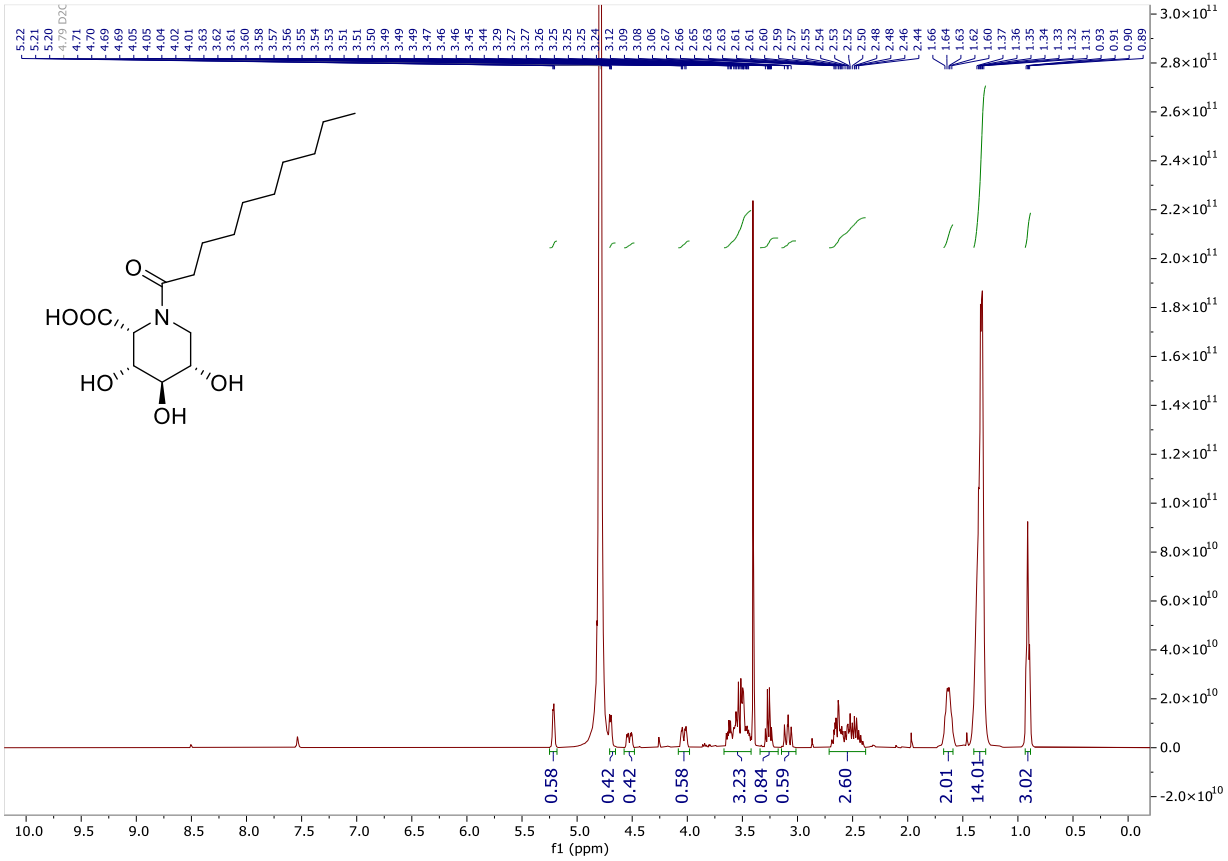

^{13}C-NMR, 101 MHz, D_2O

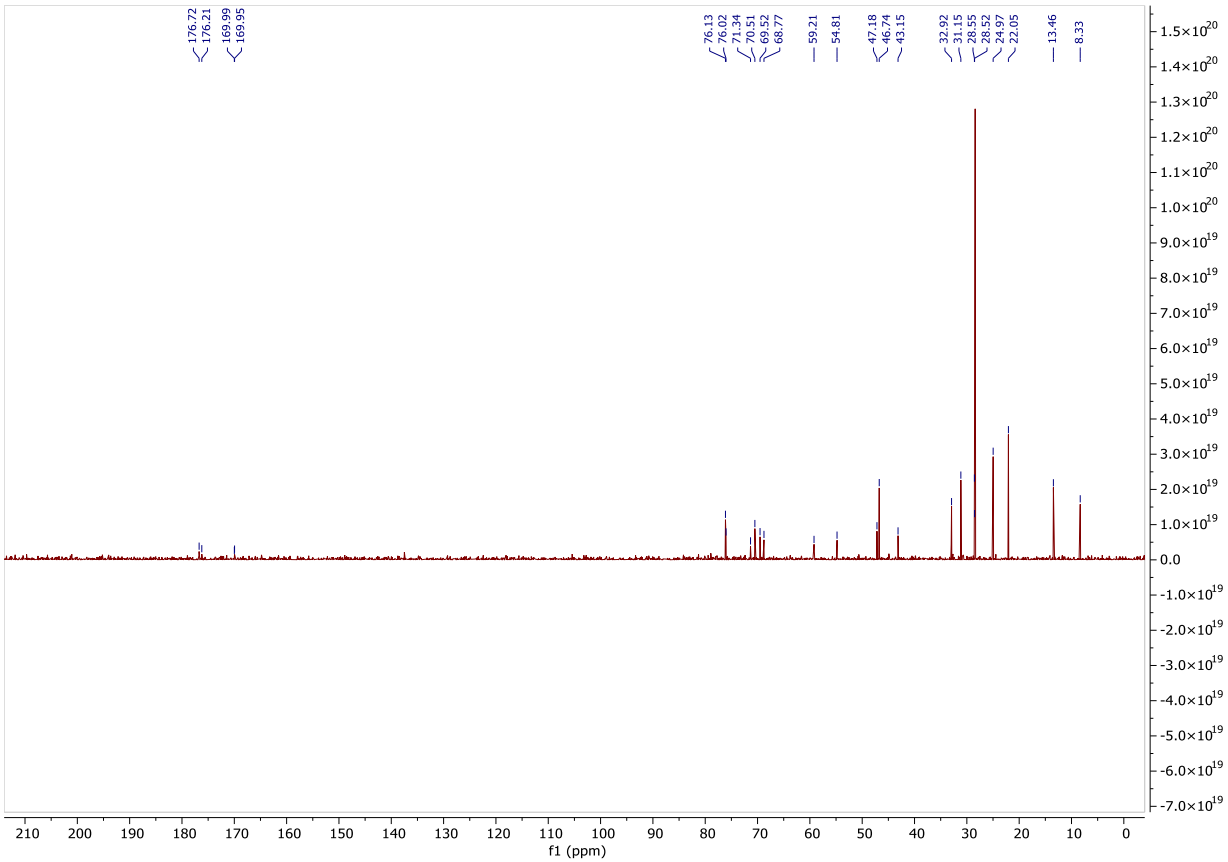

Table S1. Relative Gibbs energy calculated using the polarizable continuum solvent model PCM, equilibrium percentages at 298 K, and selected geometrical data of the B3LYP/6-311+G(d) calculated minimum energy conformations of compounds **1** and **2**.

	ΔG	**%**	**ring**	**τ_{1OH}**	**τ_{2OH}**	**τ_{3OH}**	**τ_4**
1Aa	4.49	0.0	$^4C_1$	-177	-174	146	64
1Ab	2.24	0.9	$^4C_1$	178	-175	148	-50
1Ac	6.90	0.0	$^4C_1$	-177	-176	156	-132
1Ba	4.41	0.0	$^4C_1$	89	-69	52	63
1Bb	2.41	0.7	$^4C_1$	90	-65	55	-50
1Aa_i	0.07	36,1	$^1C_4$	-91	-157	-169	63
1Ab_i	0.00	40.9	$^1C_4$	-93	-159	106	-54
1Ac_i	2.08	1.2	$^1C_4$	-95	-161	127	-177
1Ba_i	2.61	0.5	$^1C_4$	80	-80	-44	43
1Bb_i	0.45	19.2	$^1C_4$	83	-80	-31	-51
1Bc_i	2.79	0.4	$^1C_4$	85	82	91	-178
	ΔG	**%**	**ring**	**τ_{1OH}**	**τ_{2OH}**	**τ_{3OH}**	**τ_4**
2Aa	6.51	0.0	$^4C_1$	-177	-173	150	44
2Ab	6.83	0.0	$^4C_1$	180	-176	142	-39
2Ac	5.07	0.0	$^4C_1$	180	-179	153	-169
2Ba	6.77	0.0	$^4C_1$	91	-68	51	47
2Bb	6.59	0.0	$^4C_1$	90	-69	50	-40
2Bc	5.52	0.0	$^4C_1$	90	-66	50	169
2Ab_i	1.55	4.5	$^1C_4$	-93	-156	107	-5
2Ac_i	0.63	21.5	$^1C_4$	-92	-156	104	179
2Ba_i	0.97	12.1	$^1C_4$	84	-82	-29	1
2Bc_i	0.00	61.9	$^1C_4$	85	-82	-31	-178

[a] τ_{1OH}: -C1-C2-O-H. [b] τ_{2OH}: -C2-C3-O-H. [c] τ_{3OH}: -C3-C4-O-H. [d] τ_4: =N–C5-C(O)-O(H) for **2** and N–C5-C(H_2)-O(H) for **1**.

Table 1 shows that the minimum energy conformers of the two compounds, **2Bc_i** and **1Ab_i**, still assume the $^1C_4$ conformation. It is worthy pointing out that, being these compounds deoxy derivatives at the C1 of the reference compounds, any stabilization due to the anomeric effect is lost.

Table S2. Relative Gibbs energy calculated using the polarizable continuum solvent model PCM, equilibrium percentages at 298 K, and selected geometrical data of the B3LYP/6-311+G(d) calculated minimum energy conformations of compounds **3** and **4**.

	ΔG	**%**	**ring**	**τ_{1OH}**	**τ_{2OH}**	**τ_{3OH}**	**τ_4**
3Aa	1.96	2.4	$^4C_1$	-176	179	-78	65
3Ab	0.76	18.5	$^4C_1$	-178	175	157	-79
3Ac	0.00	66.8	$^4C_1$	-177	173	-95	-175
3Ba	1.92	2.6	$^4C_1$	79	-62	50	65
3Bb	1.15	9.6	$^4C_1$	80	-60	51	-76
3Aa_i	5.23	0.0	$^1C_4$	179	-176	-155	58
3Ab_i	7.85	0.0	$^1C_4$	176	-173	151	-89
3Ac_i	6.95	0.0	$^1C_4$	175	-175	164	157
3Ba_i	9.68	0.0	$^1C_4$	56	-64	53	49
3Bb_i	7.60	0.0	$^1C_4$	57	-63	66	-90
3Bc_i	7.78	0.0	$^1C_4$	57	-63	74	176
	ΔG	**%**	**ring**	**τ_{1OH}**	**τ_{2OH}**	**τ_{3OH}**	**τ_4**
4Ab	0.11	33.3	$^4C_1$	-178	175	-78	-26
4Ac	0.78	10.8	$^4C_1$	-179	172	-83	178
4Ba	0.57	15.5	$^4C_1$	81	-62	50	61
4Bb	0.00	40.4	$^4C_1$	81	-62	49	-118
4Aa_i	7.18	0.0	$^1C_4$	-83	-167	177	122
4Ab_i	6.50	0.0	$^1C_4$	-83	-167	179	-63
4Bb_i	7.04	0.0	$^1C_4$	60	-69	-38	-33
4Bc_i	6.96	0.0	$^1C_4$	61	-68	-40	172

[a] τ_{1OH}: -C1-C2-O-H. [b] τ_{2OH}: -C2-C3-O-H. [c] τ_{3OH}: -C3-C4-O-H. [d] τ_4: =N–C5-C(O)-O(H) for **3** and N–C5-C(H_2)-O(H) for **4**.

Table S3a. Relative Gibbs energy calculated using the polarizable continuum solvent model PCM, equilibrium percentages at 298 K, and selected geometrical data of the B3LYP/6-311+G(d) calculated minimum energy conformations of compound **5**.

	ΔG	%	ring	τ_{1OH}	τ_{2OH}	τ_{3OH}	τ_4	τ_5
5Aa_Z	1.27	2.9	$^4C_1$	-174	-179	154	65	-180
5Ab_Z	0.93	5.1	$^4C_1$	-177	178	156	-65	179
5Ac_Z	0.60	8.9	$^4C_1$	-176	173	-94	-177	180
5Ba_Z	1.44	2.2	$^4C_1$	83	-63	50	65	180
5Bb_Z	0.93	5.1	$^4C_1$	83	-62	52	-63	179
5Bc_Z	0.00	24.4	$^4C_1$	84	-63	46	-165	-179
5Aa_E	1.94	0.9	$^4C_1$	-175	-179	152	64	1
5Ab_E	0.51	10.4	$^4C_1$	-177	178	154	-65	3
5Ac_E	0.58	9.2	$^4C_1$	-177	174	-93	-177	1
5Ba_E	1.75	1.3	$^4C_1$	80	-63	50	64	1
5Bb_E	0.61	8.7	$^4C_1$	80	-61	52	-63	3
5Bc_E	0.09	21.1	$^4C_1$	81	-63	46	-164	2
5Aa_Z_i	10.09	0.0	$^1C_4$	-171	-172	-173	92	-178
5Ab_Z_i	13.94	0.0	$^1C_4$	-77	-180	81	-104	-175
5Ac_Z_i	7.07	0.0	$^1C_4$	161	-170	-46	-160	-179
5Ba_Z_i	6.17	0.0	$^1C_4$	70	-74	-42	81	179
5Bb_Z_i	5.02	0.0	$^1C_4$	70	-74	-45	-62	-178
5Bc_Z_i	9.99	0.0	$^1C_4$	79	-66	62	-160	-178
5Aa_E_i	11.94	0.0	$^1C_4$	-174	-171	-180	89	-2
5Ac_E_i	9.98	0.0	$^1C_4$	160	-170	-42	-159	-1
5Ba_E_i	13.18	0.0	$^1C_4$	20	-73	-33	92	34

[a] τ_{1OH}: -C1-C2-O-H. [b] τ_{2OH}: -C2-C3-O-H. [c] τ_{3OH}: -C3-C4-O-H. [d] τ_4: = N–C5-C(H_2)-O(H) for **6**. [e] τ_5: C5-N-C(=O)-C for **5**.

Table S3b. Relative Gibbs energy calculated using the polarizable continuum solvent model PCM, equilibrium percentages at 298 K, and selected geometrical data of the B3LYP/6-311+G(d) calculated minimum energy conformations of compound **6**.

	ΔG	**%**	**ring**	**τ_{1OH}**	**τ_{2OH}**	**τ_{3OH}**	**τ_4**	**τ_5**
6Aa_Z	0.62	12.2	$^4C_1$	-175	-178	155	50	180
6Ac_Z	0.00	34.4	$^4C_1$	-175	-178	157	-137	180
6Aa_E	1.43	3.1	$^4C_1$	-175	-176	152	55	3
6Ac_E	0.77	9.3	$^4C_1$	-175	-177	154	-132	3
6Ba_Z	0.75	9.7	$^4C_1$	85	-62	50	54	180
6Bc_Z	0.25	22.6	$^4C_1$	84	-62	49	-129	180
6Ba_E	1.79	1.7	$^4C_1$	82	-62	49	-69	3
6Bc_E	0.94	7.0	$^4C_1$	82	-62	49	-124	3
6Aa_Z_i	5.28	0.0	$^1C_4$	-82	-165	-167	63	173
6Ab_Z_i	6.69	0.0	$^1C_4$	-84	-165	80	34	175
6Ac_Z_i	4.52	0.0	$^1C_4$	-82	-165	-165	-119	174
6Ab_E_i	10.78	0.0	$^1C_4$	-178	-168	162	-58	4
6Ba_Z_i	6.39	0.0	$^1C_4$	59	-74	-49	35	174
6Bc_Z_i	6.20	0.0	$^1C_4$	59	74	-48	-151	175
6Ba_E_i	8.99	0.0	1C4	57	-48	-46	30	-7
6Bc_E_i	7.71	0.0	1C4	56	-73	-56	-156	-6

[a] τ_{1OH}: -C1-C2-O-H. [b] τ_{2OH}: -C2-C3-O-H. [c] τ_{3OH}: -C3-C4-O-H. [d] τ_4: =N–C5-C(O)-O(H). [e] τ_5: C5-N-C(=O)-C

Tables S4: Predicted chemical shifts (δ) determined through GIAO NMR calculations at the B3LYP/6-311+G(d) of the H and C atoms (*δ*, in ppm relative to TMS) of compounds **1-6** on the basis of the geometries optimized at the same level, and experimental NMR data recorded in D_2O or MeOD as specified, at 298 K if not differently stated.

	Compound 1 ($^1C_4$)						
	H1(ax)	**H1(eq)**	**H2**	**H3**	**H4**	**H5**	**H6a,b**
Calculated	3,86	3,58	4,44	4,62	4,47	3,83	4.22/4.21
Found MeOD	3,39/3,25	3,39/3,25	3,97	3,97	3,92	3,50	3,88/3,83

	Compound 2 ($^1C_4$)					
	H1(ax)	**H1(eq)**	**H2**	**H3**	**H4**	**H5**
Calculated	3,92	3,38	4,30	4,63	5,01	4,46
Found D_2O	3.50 – 3.39		4.09-4.05	4.11	4.40	4.30

	Compound 3 ($^4C_1$)						
	H1(ax)	**H1(eq)**	**H2**	**H3**	**H4**	**H5**	**H6a,b**
Calculated	2,37	2,92	3,90	3,72	3,86	3,36	4.06/4.30
Found MeOD	2.77	2.96	3.65	3.52	3.79	3.15	3.95 – 3.83

	Compound 4 ($^4C_1$)					
	H1(ax)	**H1(eq)**	**H2**	**H3**	**H4**	**H5**
Calculated	2,85	2,84	3,82	3,71	3,91	3,76
Found D_2O[a]	3,10	2,90	3,70	3,86	3,59	3,64

[a]310K, 600 MHz

		Compound 5 ($^4C_1$)						
		H1(ax)	**H1(eq)**	**H2**	**H3**	**H4**	**H5**	**H6a,b**
Calculated	(E)	2,49	4,80	3,57	3,85	3,92	4,26	3.81/4.32
Found (MeOD)		2,64	4,62	3,28	3,39	3,53	4,24	3,85-3,95
Calculated	(Z)	3,03	3,45	3,60	3,98	3,90	5,43	3.78/4.22
Found (MeOD)		3,16	3,83	3,37	3,52	3,45	4,97	3,85-3,95

		Compound 6 ($^4C_1$)					
		H1(ax)	**H1(eq)**	**H2**	**H3**	**H4**	**H5**
Calculated	*(Z)*	3,92	3,57	3,71	4,20	3,77	5,10
Found D_2O		3,00	3,94	3,48	3,42	3,39	5,12
Calculated	(*E*)	3,36	4,79	3,60	4,29	3,83	4,61
Found D_2O		2,53	4,44	3,36	3,40	3,54	4,61

	Compound 1 ($^1C_4$)					
	C1	**C2**	**C3**	**C4**	**C5**	**CH_2OH**
Calculated	54,5	72,9	70,8	78,2	63,2	68,0
Found MeOD	47.01	69.21, 68.36, 67.85			58.28	60.65

	Compound 2 ($^1C_4$)					
	C1	**C2**	**C3**	**C4**	**C5**	**COOH**
Calculated	52,6	73,9	70,7	76,5	65,0	172,3
Found D_2O	45.09	68.37, 67.22, 65.74			57.81	171.09

	Compound 3 ($^4C_1$)						
	C1	**C2**	**C3**	**C4**	**C5**	**CH_2OH**	**CN**
Calculated	52,5	77,1	82,8	81,1	67,0	63,6	60,6
Found MeOD	55.44/53.13	74.22, 72.60, 70.70			63,96	58.32,	55.44/53.13

	Compound 4 ($^4C_1$)						
	C1	**C2**	**C3**	**C4**	**C5**	**COOH**	**CN**
Calculated	52,4	77,3	81,9	78,8	71,2	182,2	60,6
Found	57.92	77.99	80.57	76.23	72.51	ND	61.05

		Compound 5 ($^4C_1$)						
		C1	**C2**	**C3**	**C4**	**C5**	**CH_2OH**	**CONR**
Calculated	(E)	43,7	76,8	81,1	79,1	60,9	65,1	178,0
Found (MeOD)	(E)	40.31	74.91, 74.82, 71.36, 70.69, 69.81, 56.54			59.76	56.54, 55.73	174.47, 174.15
	(Z)	45.35,				54.36		
Calculated	(Z)	49,6	77,2	81,1	78,8	54,8	65,5	177,0

		Compound 6 ($^4C_1$)						
		C1	**C2**	**C3**	**C4**	**C5**	**COOH**	**CONR**
Calculated	(E)	44,2	76,0	79,7	77,6	63,6	176,8	177,6
Found (MeOD)	(E)	43,15	76.13, 76.02, 71.34, 70.51, 69.52, 68.77			59.21	176.72, 176.21	169.99, 169.95
	(Z)	47,18				54.81		
Calculated	(Z)	49,2	76,1	79,7	76,9	58,5	178,2	170,3

Figure S1: Details of ^{1}H NMR of compounds **1** (d_4 MeOD) and **2** (D_2O): diagnostic coupling constants of the $^1C_4$ conformation.

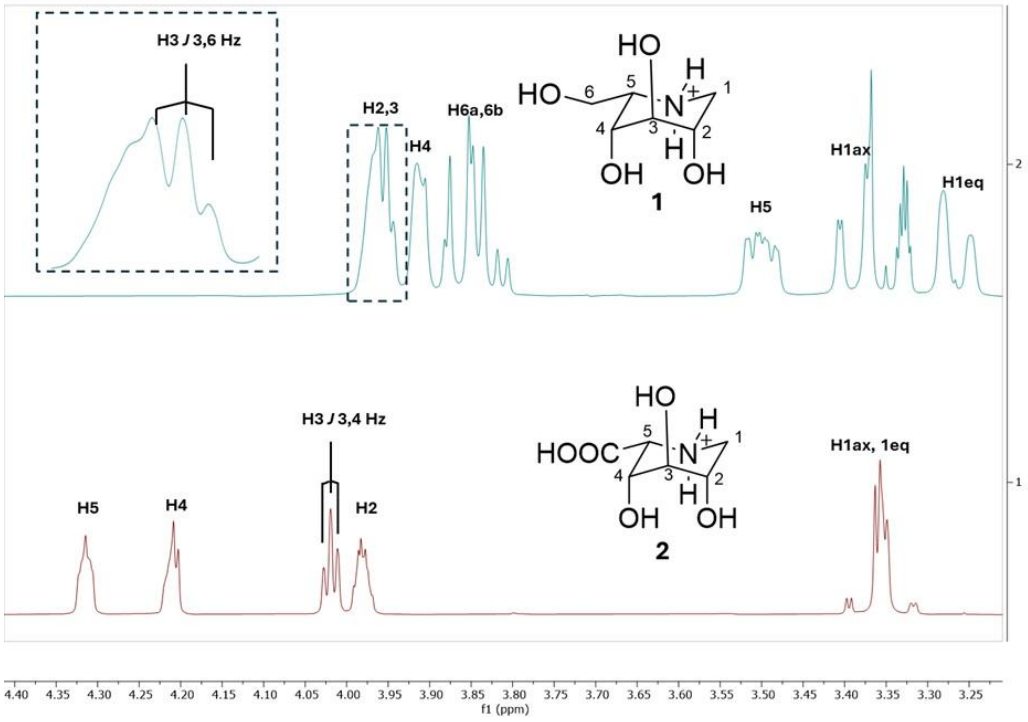

Figure S2: Electrostatic surface representation of the most stable conformations of compounds **3** (A) and **4** (B) in transparent (left) and solid (right) representation.

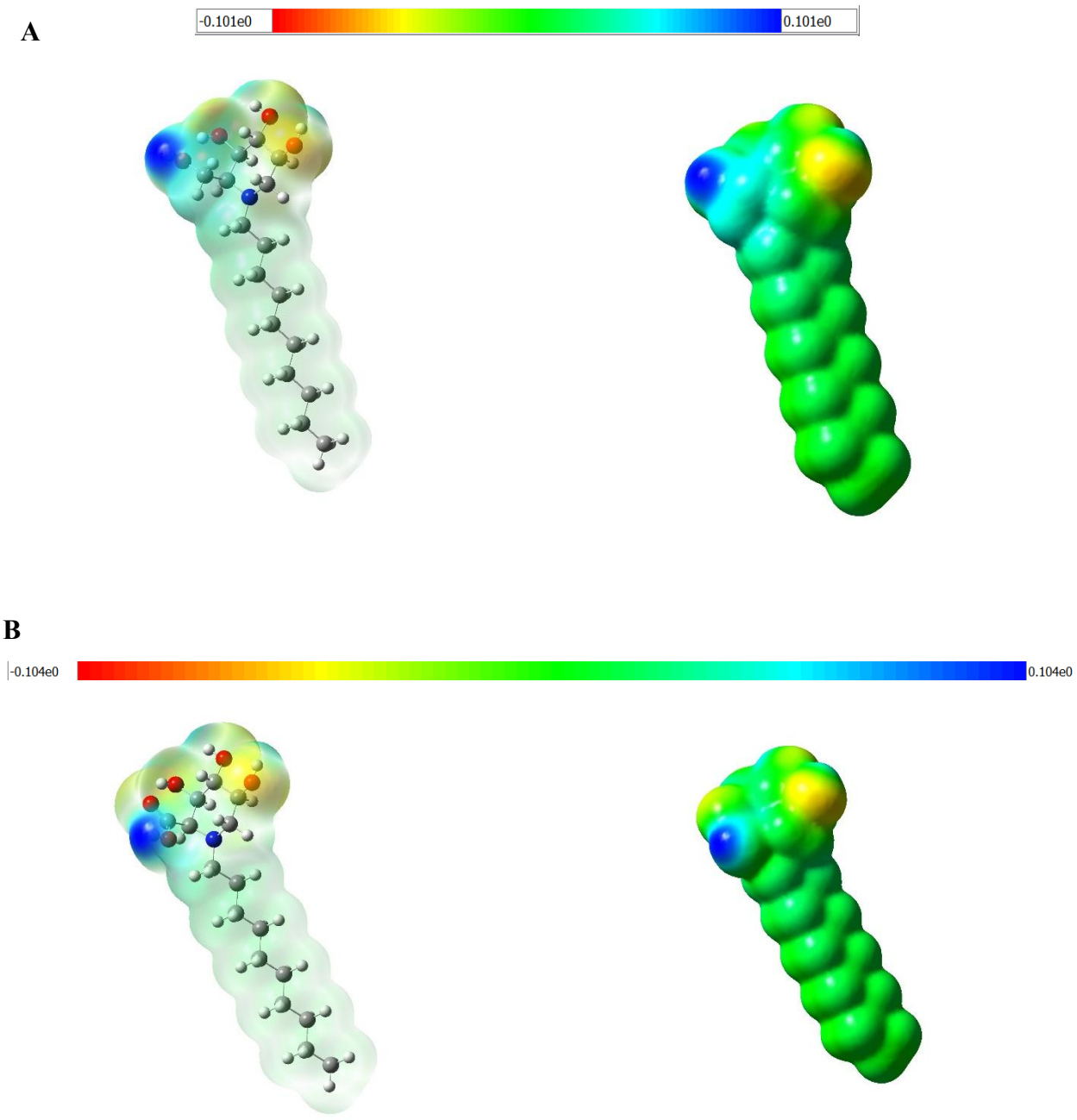

Figure S3: Electrostatic surface representation of the most stable conformations of L-Idose (C) and L-iduronic acid (D) in transparent (left) and solid (right) representation.

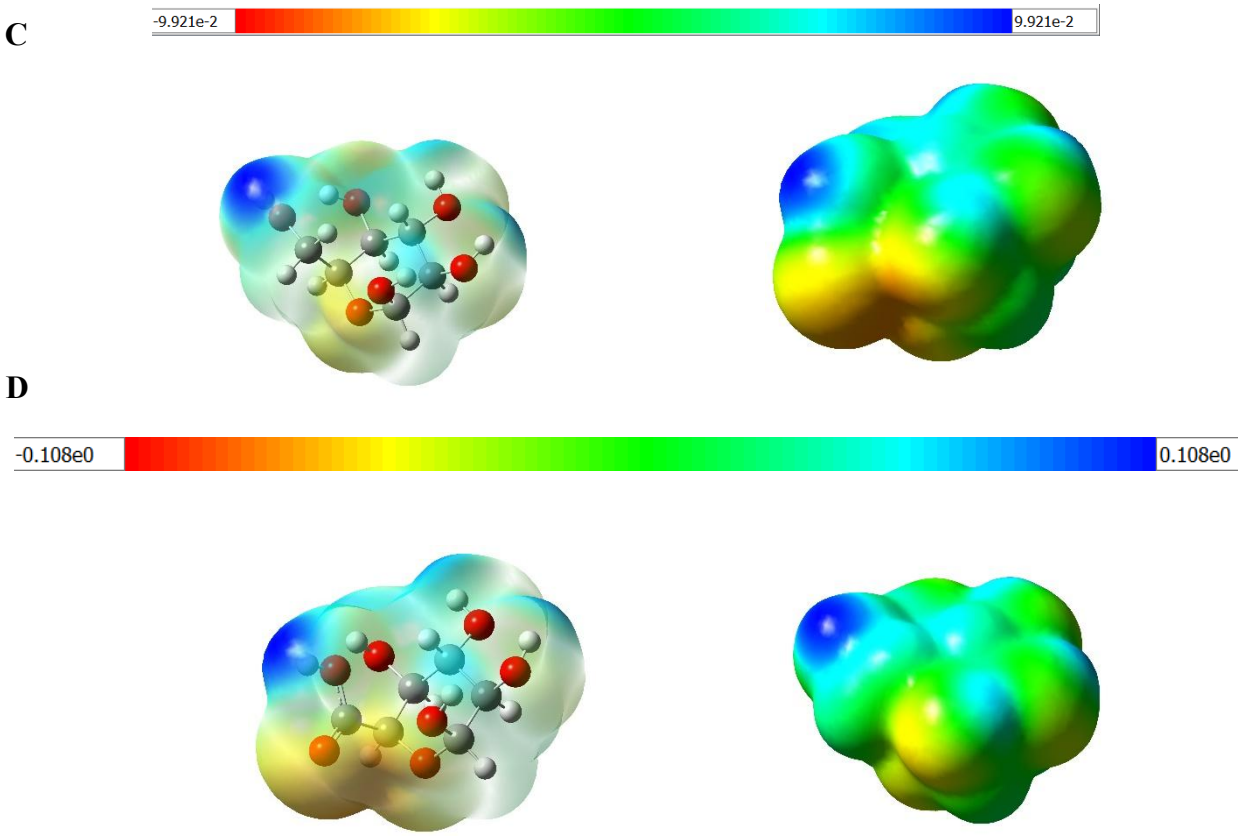

Molecular Dynamic (MD) simulations

Methods

MD simulations of compounds **3** and **4**, without simplification of the alkyl chain and as model structures of the two series of synthesized analogues, were performed with the SANDER module of the AMBER20 package[1] along with the general amber force field (gaff)[2] and AM1-*BCC* atomic charges[3,4] The TIP3P model[5] was employed to explicitly represent water molecules. Compound **3** and **4** were immersed in a box containing 4255, and 4275 water molecules, respectively. A minimization of the whole system was performed by setting a convergence criterion on the gradient of 10^{-4} kcal mol^{-1} $Å^{-1}$. Prior to starting the MD simulations, the system was equilibrated for 2 ns at 310 K in isocore conditions (NVT). Subsequently, 100 ns of MD simulations in an isothermal-isobaric ensemble were carried out at 310 K with a 2 fs time-step (NPT). In the production runs, the systems were performed in periodic boundary conditions. Van der Waals and short-range electrostatic interactions were estimated within a 20 Å cutoff. VMD 1.9.3 was used for molecular visualization and for animating trajectory data. The MD trajectory frames were analyzed by clustering the conformations adopted by **3** and **4**. The cluster analysis was performed using the *cpptraj* module[6] of AMBER20. By this algorithm, the MD frames were divided into clusters by the complete average linkage algorithm, and the conformations with the lowest root mean square deviation (RMSD) to the cluster centers (the structures representative of the cluster, SRC) were acquired and visually inspected.

Molecular Dynamics (MD) simulations were performed for 100 ns using explicit water as solvent and a cluster analysis was carried out, locating the different conformational families describing the structures. For **3**, only two geometries resulted to be populated for more than 10%, accounting together the 80% of the overall population. They are reported in Figure S4.

For compound **4**, three geometries resulted to be populated for more than 10%, accounting together about 88% of the overall population. They are reported in Figure S5.

Figure S4. 3D-plots of the most populated conformational families c0 (43.5%) and c1 (36.5%) of **3** from MD simulations.

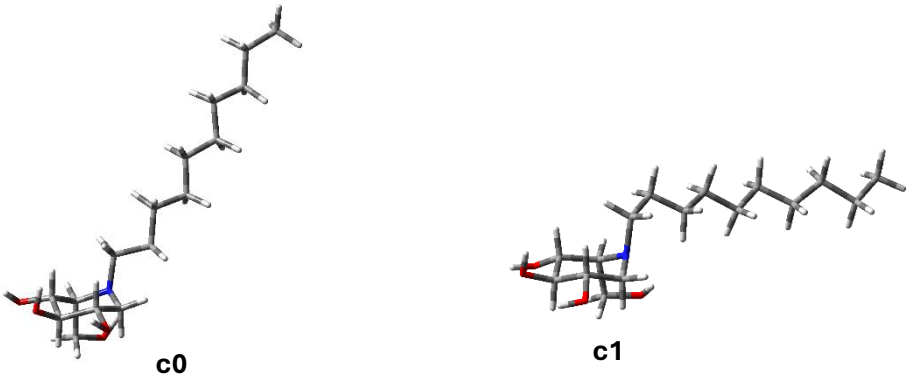

Figure S5: 3D-plots of the most populated conformational families c0 (38.8%), c1 (35.9%) and c2 (13.4%) of 4 from MD simulations

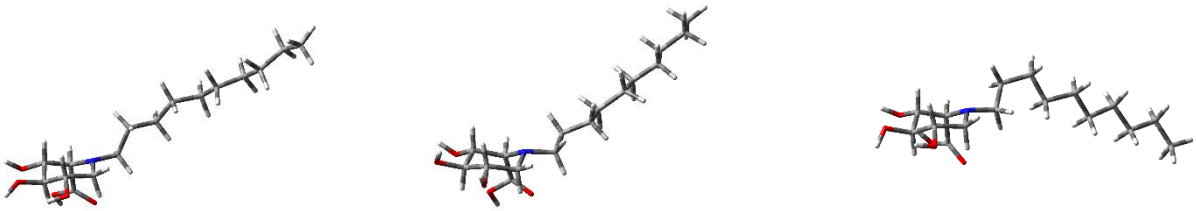

References

1) D. A. Case, H. M. Aktulga, K. Belfon, I. Y. Ben-Shalom, S. R. Brozell, D. S. Cerutti, T. E. Cheatham, V. W. D. Cruzeiro, T. A. Darden, R. E. Duke, et al., Amber 2021. University of California: San Francisco, CA, USA, 2021.
2) J. Wang, R.M. Wolf, J.W. Caldwell, P.A. Kollman, D.A. Case, *J. Comp. Chem*. 2004, **25 (9)**, 1157–1174.
3) A. Jakalian, B.L. Bush, D.B. Jack, C.I. Bayly *Method*. 2000, **21 (2)**, 132–146,
4) W. Humphrey, A. Dalke, K. Schulten, *J. Mol. Graph*. 1996, **14 (1)**, 33–38.
5) W.L. Jorgensen, J. Chandrasekhar, J.D. Madura, R.W. Impey, M.L. Klein, *J. Chem. Phys*. 1983, **79**, 926–935.
6) D.R. Roe, T.E. Cheatham III, *J. Chem. Theory Comput*. 2013, **9 (7**), 3084–3095.